

Direct Urca processes involving singlet proton superfluidity in neutron star cooling

Yan Xu,^{1,*} Xiu Lin Huang,² Xiao Jun Zhang,¹ Tmurbagan Bao,³ Lin Xiao,¹ Cun Bo Fan,¹ and Cheng Zhi Liu^{1,†}

¹*Changchun Observatory, National Astronomical Observatories, CAS, Changchun 130117, China*

²*Center for Theoretical Physics, Jilin University, Changchun 130012, China*

³*College of Physics and Electronic Information, Inner Mongolia University for the Nationalities, Tongliao 028043, China*

(Dated: June 30, 2021)

A detailed description of the baryon direct Urca processes A: $n \rightarrow p + e + \bar{\nu}_e$, B: $\Lambda \rightarrow p + e + \bar{\nu}_e$, C: $\Xi^- \rightarrow \Lambda + e + \bar{\nu}_e$ related to the neutron star cooling is given in the relativistic mean field approximation. The contributions of the reactions B and C on the neutrino luminosity are calculated by means of the relativistic expressions of the neutrino energy losses. Our results show that the total neutrino luminosities of the reactions A, B, C within the mass range $1.603\text{--}2.067M_\odot$ ($1.515\text{--}1.840M_\odot$ for TM1 model) for GM1 model are larger than the corresponding values for neutron stars in $npe\mu$ matter. Although the hyperon direct Urca processes B and C reduce the neutrino emissivity of the reaction A, it illustrates the reactions B and C still make the total neutrino luminosity enhancement in the above mentioned areas. Furthermore, when we only consider the 1S_0 proton superfluidity in neutron star cooling, we find that although the neutrino emissivity of the reactions A and B is suppressed with the appearance of 1S_0 proton superfluidity, the total contribution of the reactions A, B, C can still quicken a massive neutron star cooling. These results could be used to help prove appearing hyperons in PSR J1614-2230 and J0348+0432 from neutron star cooling perspective.

PACS numbers: 21.60.-n, 26.60.-c, 26.60.Dd, 24.10.Jv, 13.75.Cs

I. INTRODUCTION

Neutron star (NS) constitutes one of the best astrophysical laboratories for studying dense matter physics. It arises at the end of life of a $8\text{--}20 M_\odot$ massive stars and forms in the aftermath of the core collapse supernovae explosion. A newly born NS is very hot with temperature as high as $10^{11}\text{--}10^{12}\text{K}$, but rapidly cools to a temperature of less than 10^{10}K within minutes. The cooling process of a NS is dominated by a combination of surface photon emission and interior neutrino emission. The latter is responsible for about $10^5\text{--}10^6$ years until the interior temperature reaches 10^6K . It is generally known that photon luminosity is obviously lower than neutrino luminosity, meaning that the thermal radiation from a NS surface reflects the intensity of interior neutrino emission[1, 2]. While neutrino emission depends strongly on the composition of superdense matter in NSs. It is well known that NSs cores are dense enough to allow for emerging exotic matter with the strangeness quantum number through weak equilibrium, such as Λ , Σ^0 , Σ^+ , Σ^- , Ξ^0 , Ξ^- hyperons, referred as $npe\mu$ matter, except for the conventional nucleons and leptons ($npe\mu$ matter)[3–10]. It means that all the possible baryon neutrino emission processes would happen during the neutrino cooling stage [11–20]. Among them, the most powerful enhancement of neutrino emission is provided by the nucleon direct Urca processes (NDUP), secondarily is the hyperon direct Urca processes (HDUP) [21–28]. Besides, the degrees of freedom of hyperons tend to soften the equation of state (EOS) calculated in the relativistic mean field (RMF)

model based on SU(6) spin-flavor symmetry (quark model for the vector meson-hyperon coupling constants), then reduce the maximum mass of NS to about $1.6\text{--}1.7M_\odot$ [29–35]. However, Demorest et al. in 2010[36] indicated that the binary millisecond pulsar PSR J1614-2230 expanded the maximum observational mass from $1.67 \pm 0.02M_\odot$ to $1.97 \pm 0.04M_\odot$ using the Shapiro delay measurements from radio timing observations. Antoniadis et al. in 2013[37] observed another massive neutron star PSR J0348+0432, whose mass is $2.01 \pm 0.04M_\odot$. It is clear that the inclusion of hyperons in such heavy NS cores are difficult to explain by SU(6) spin-flavor symmetry in RMF model. And for this reason, the SU(3) flavor symmetry is widely applied to RMF model. Because it changes the strength of the isoscalar, vector-meson(ω and ϕ) couplings to the octet states, which can sustain a NS with mass of $(1.8\text{--}2.1)M_\odot$ even if hyperons exist in NS core [38–41]. Furthermore, baryons in NS interior can become the superfluid state related to the generation of BB Cooper pairs under attractive interaction. The baryon superfluidity(SF) could suppress considerably the NDUP, HDUP and thus affect the cooling rate of NS remarkably [4, 24, 42]. As we all know, the neutrons in the crust and protons, hyperons in the core undergo Cooper pair in 1S_0 state, while neutrons in the core can pair in 3P_2 state.

This paper is arranged as follows. In section 2, we make a brief review for RMF, NS cooling theories and the gap equation for the 1S_0 proton SF. The numerical results are discussed in section 3. Finally, we summarize our conclusions in section 4.

* Corresponding E-mail: xuy@cho.ac.cn

† Corresponding E-mail: lcz@cho.ac.cn

	$g_{\sigma N}$	$a(fm^{-1})$	b	c_3	$g_{\omega N}$	$g_{\rho N}$	$g_{\phi N}$	$g_{\sigma\Lambda}$	$g_{\sigma\Sigma}$	$g_{\sigma\Xi}$	$g_{\sigma^*\Lambda}$	$g_{\sigma^*\Xi}$
GM1 SU(6)	9.57	12.28	-8.98	0	10.61	4.10	-	5.84	3.87	3.06	3.73	9.67
GM1 SU(3)	9.57	12.28	-8.98	0	10.26	4.10	-3.50	7.25	5.28	5.87	2.60	6.82
TM1 SU(6)	10.029	7.233	0.618	71.308	12.614	4.632	-	6.17	4.472	3.202	5.015	11.516
TM1 SU(3)	10.029	7.233	0.618	81.601	12.199	4.640	-4.164	7.733	6.035	6.328	3.691	8.100

TABLE I. The parameter sets GM1 and TM1. The relations, $g_{\sigma^*N} = g_{\rho\Lambda} = 0$, are assumed. We take $m_\omega = 783\text{MeV}$, $m_\rho = 770\text{MeV}$, $m_N = 938\text{MeV}$. For the GM1 and TM1 models, $m_\sigma = 550\text{MeV}$ and 511.198MeV , respectively.

	$g_{\omega\Lambda}$	$g_{\omega\Sigma}$	$g_{\omega\Xi}$	$g_{\phi\Lambda}$	$g_{\phi\Sigma}$	$g_{\phi\Xi}$
GM1 SU(6)	7.073	7.073	3.537	5.002	5.002	10.003
GM1 SU(3)	8.149	8.149	6.038	-6.253	-6.253	-9.004
TM1 SU(6)	8.409	8.409	4.205	5.945	5.945	11.891
TM1 SU(3)	9.689	9.689	7.180	-7.435	-7.435	-10.706

TABLE II. The other coupling constants for hyperons. The relations, $g_{\rho N} = \frac{1}{2}g_{\rho\Sigma} = g_{\rho\Xi}$, are assumed.

II. THE DENSITY EQUATIONS

A. RMF Theory

In this calculation, we adopt RMF model to describe NS matter. The constituents of NSs fall into two categories: $npe\mu$ and $nphe\mu$ matter. The strong interaction between baryons is mediated by the exchange of isoscalar scalar and vector mesons σ , ω , isovector vector meson ρ . The two additional strange mesons are also included, namely isoscalar scalar σ^* and vector ϕ mesons [33, 34, 43]. The total Lagrangian is given by

$$\begin{aligned}
L = & \sum_B \bar{\psi}_B [i\gamma_\mu \partial^\mu - (m_B - g_{\sigma B}\sigma - g_{\sigma^* B}\sigma^*)] \\
& - g_{\rho B}\gamma_\mu \tau \cdot \rho^\mu - g_{\omega B}\gamma_\mu \omega^\mu - g_{\phi B}\gamma_\mu \phi^\mu \psi_B \\
& + \frac{1}{2}(\partial_\mu \sigma \partial^\mu \sigma - m_\sigma^2 \sigma^2) + \frac{1}{2}(\partial_\nu \sigma^* \partial^\nu \sigma^* - m_{\sigma^*}^2 \sigma^{*2}) \\
& - \frac{1}{4}W^{\mu\nu}W_{\mu\nu} - \frac{1}{4}R^{\mu\nu}R_{\mu\nu} - \frac{1}{4}P^{\mu\nu}P_{\mu\nu} + \frac{1}{2}m_\omega^2 \omega_\mu \omega^\mu \\
& + \frac{1}{2}m_\rho^2 \rho_\mu \rho^\mu + \frac{1}{2}m_\phi^2 \phi_\mu \phi^\mu + \frac{1}{4}c_3(\omega_\mu \omega^\mu)^2 \\
& - \frac{1}{3}a\sigma^3 - \frac{1}{4}b\sigma^4 + \sum_l \bar{\psi}_l [i\gamma_\mu \partial^\mu - m_l]\psi_l.
\end{aligned} \quad (1)$$

Here $W_{\mu\nu} = \partial_\mu \omega_\nu - \partial_\nu \omega_\mu$, $R_{\mu\nu} = \partial_\mu \rho_\nu - \partial_\nu \rho_\mu$ and $P_{\mu\nu} = \partial_\mu \phi_\nu - \partial_\nu \phi_\mu$ denote the field tensors of ω , ρ and ϕ mesons, respectively. The sum on B and l runs over the octet baryons and leptons, namely, n, p, Λ , Σ^0 , Σ^+ , Σ^- , Ξ^0 , Ξ^- , e, μ . ψ_B , ψ_l and m_B , m_l are the baryon, lepton Dirac fields and masses, respectively. γ_u is the Dirac matrix. The meson fields are replaced by their expectation values at the mean field level. Now we are going to plug the

above Lagrangian into the Euler-Lagrange equations

$$\frac{\partial L}{\partial \psi(x)} - \partial_\mu \frac{\partial L}{\partial (\partial_\mu \psi)} = 0 \quad (2)$$

The equations of motion for each baryon and meson fields can be obtained in RMF approximation

$$(i\gamma_\mu \partial^\mu - m_B^* - g_{\omega B}\gamma_0 \omega^0 - g_{\rho B}\gamma_0 \tau_3 \rho_3^0 - g_{\phi B}\gamma_0 \phi^0)\psi_B = 0, \quad (3)$$

$$\sum_B g_{\sigma B}\rho_{SB} = m_\sigma^2 \sigma + a\sigma^2 + b\sigma^3, \quad (4)$$

$$\sum_B g_{\omega B}\rho_B = m_\omega^2 \omega_0 + c_3 \omega_0^3, \quad (5)$$

$$\sum_B g_{\rho B}\rho_B I_{3B} = m_\rho^2 \rho_03, \quad (6)$$

$$\sum_B g_{\sigma^* B}\rho_{SB} = m_{\sigma^*}^2 \sigma^*, \quad (7)$$

$$\sum_B g_{\phi B}\rho_B = m_\phi^2 \phi_0. \quad (8)$$

Here J_B and I_{3B} express the baryon spin and isospin projections, respectively. m_B^* is the baryon effective mass

$$m_B^* = m_B - g_{\sigma B}\sigma - g_{\sigma^* B}\sigma^*, \quad (9)$$

The scalar density ρ_{SB} and baryon density ρ_B are given by

$$\rho_{SB} = \frac{2J_B + 1}{2\pi^2} \int_0^{p_{FB}} \frac{m_B^*}{\sqrt{p_B^2 + m_B^{*2}}} p_B^2 dp_B \quad (10)$$

$$\rho_B = \frac{1}{\pi^2} \int_0^\infty dp_B p_B^2. \quad (11)$$

Processes	Transition	C	f_1	g_1
A	$n \rightarrow p + e + \bar{\nu}_e, p + e \rightarrow n + \nu_e$	$\cos \theta_C$	1	F+D
B	$\Lambda \rightarrow p + e + \bar{\nu}_e, p + e \rightarrow \Lambda + \nu_e$	$\sin \theta_C$	$-\sqrt{3/2}$	$-\sqrt{3/2}(F + D/3)$
C	$\Xi^- \rightarrow \Lambda + e + \bar{\nu}_e, \Lambda + e \rightarrow \Xi^- + \nu_e$	$\sin \theta_C$	$\sqrt{3/2}$	$\sqrt{3/2}(F - D/3)$
D	$\Xi^- \rightarrow \Xi^0 + e + \bar{\nu}_e, \Xi^0 + e \rightarrow \Xi^- + \nu_e$	$\cos \theta_C$	1	F-D
E	$\Sigma^- \rightarrow n + e + \bar{\nu}_e, n + e \rightarrow \Sigma^- + \nu_e$	$\sin \theta_C$	-1	D-F
F	$\Sigma^- \rightarrow \Lambda + e + \bar{\nu}_e, \Lambda + e \rightarrow \Sigma^- + \nu_e$	$\cos \theta_C$	0	$\sqrt{2/3}D$
G	$\Sigma^- \rightarrow \Sigma^0 + e + \bar{\nu}_e, \Sigma^0 + e \rightarrow \Sigma^- + \nu_e$	$\cos \theta_C$	$\sqrt{2}$	$\sqrt{2}F$
H	$\Xi^- \rightarrow \Sigma^0 + e + \bar{\nu}_e, \Sigma^0 + e \rightarrow \Xi^- + \nu_e$	$\sin \theta_C$	$\sqrt{1/2}$	$(F + D)/\sqrt{2}$
I	$\Xi^0 \rightarrow \Sigma^+ + e + \bar{\nu}_e, \Sigma^+ + e \rightarrow \Xi^0 + \nu_e$	$\sin \theta_C$	1	F+D

TABLE III. The constants of the baryon direct Urca processes. We take $\sin \theta_c = 0.231 \pm 0.003$, $F = 0.477 \pm 0.012$, $D = 0.756 \pm 0.011$.

The hadron phase should meet the local charge neutrality and beta-equilibrium conditions. The former is given by

$$\rho_p + \rho_{\Sigma^+} = \rho_{\Sigma^-} + \rho_{\Xi^-} + \rho_e + \rho_\mu. \quad (12)$$

The latter is imposed by the baryon chemical potential, which is a linear combination of μ_n and μ_e ,

$$\mu_B = \mu_n - q_B \mu_e, \mu_e = \mu_\mu \quad (13)$$

where q_B is the baryon electric charge (in unit of e).

We can solve the Eqs. (3)-(13) self-consistently at a given baryon density ρ_B .

The total energy density and pressure of NS matter are

$$\begin{aligned} \varepsilon = & \sum_B \frac{1}{\pi^2} \int_0^{p_{FB}} \sqrt{p_B^2 + m_B^{*2}} p_B^2 dp_B + \frac{1}{2} m_\sigma^2 \sigma^2 + \frac{1}{3} a \sigma^3 \quad (14) \\ & + \frac{1}{4} b \sigma^4 + \frac{1}{2} m_{\sigma^*}^2 \sigma^{*2} + \frac{1}{2} m_\omega^2 \omega^2 + \frac{3}{4} c_3 \omega^4 + \frac{1}{2} m_\phi^2 \phi^2 \\ & + \frac{1}{2} m_\rho^2 \rho^2 + \sum_l \frac{1}{\pi^2} \int_0^{p_{Fl}} \sqrt{p_l^2 + m_l^{*2}} p_l^2 dp_l \end{aligned}$$

$$\begin{aligned} P = & \frac{1}{3} \sum_B \frac{1}{\pi^2} \int_0^{p_{FB}} \frac{p_B^4 dp_B}{\sqrt{p_B^2 + m_B^{*2}}} - \frac{1}{2} m_\sigma^2 \sigma^2 - \frac{1}{3} a \sigma^3 \quad (15) \\ & - \frac{1}{4} b \sigma^4 - \frac{1}{2} m_{\sigma^*}^2 \sigma^{*2} + \frac{1}{2} m_\omega^2 \omega^2 + \frac{1}{4} c_3 \omega^4 + \frac{1}{2} m_\phi^2 \phi^2 \\ & + \frac{1}{2} m_\rho^2 \rho^2 + \frac{1}{3} \sum_l \frac{1}{\pi^2} \int_0^{p_{Fl}} \frac{p_l^4 dk}{\sqrt{p_l^2 + m_l^{*2}}} dp_l \end{aligned}$$

Eqs. (14) and (15) as inputs, we can obtain the mass-radius relation by solving the Tolman-Oppenheimer-Volkoff (TOV) equation [44, 45]

$$\begin{aligned} \frac{dP(r)}{dr} = & - \frac{[P(r) + \varepsilon(r)][M(r) + 4\pi r^3 P(r)]}{r(r - 2M(r))}, \quad (16) \\ \frac{dM(r)}{dr} = & 4\pi r^2 \varepsilon(r). \end{aligned}$$

We adopt two successful RMF parameter sets to describe NS matter, GM1 and TM1, as listed in Table I [39]. These parameters have been determined by fitting to some ground state properties of nuclear matter. As for the couplings of the isoscalar vector mesons ω and ϕ to baryons, we adopt two relations: SU(6) spin-flavor symmetry based on the naive quark model and general SU(3) flavor symmetry, as listed in Table II [40].

B. NS cooling theory

The baryon direct Urca processes consist of two successive reactions, beta decay and capture, are listed in Table III [22].

$$B_1 \rightarrow B_2 + e + \bar{\nu}_e, B_2 + e \rightarrow B_1 + \nu_e. \quad (17)$$

Here B_1 and B_2 represent baryons. Due to the EOSs of NSs matter are derived by RMF model, so the neutrino energy losses must be consistent with the used relativistic EOSs. In the free relativistic gas, the energy and momentum conservations require a large effective mass difference of B_1 and B_2 , $m_{B_1}^* - m_{B_2}^* \sim 100 \text{ MeV}$, which is unlikely to appear in the reactions A, D and G. The reason is that the effective masses of hyperons with the same species but the different isospins are same in Eq.(9). Therefore, in the relativistic regime, the energy conservation should be assured by considering the potential energy difference of B_1 and B_2 . The neutrino emissivity can be given by the Fermi Golden Rule

$$\begin{aligned} Q_0 = & 2 \int \left[\prod_{j=1}^4 \frac{d^3 p_j}{(2\pi)^{12} (2\varepsilon_j)} \right] \varepsilon_4 f_1 (1 - f_2) (1 - f_3) |M_{fi}|^2 \quad (18) \\ & \times (2\pi)^4 \delta(E_1 - E_2 - \varepsilon_3 - \varepsilon_4) \delta(\mathbf{p}_1 - \mathbf{p}_2 - \mathbf{p}_3 - \mathbf{p}_4), \end{aligned}$$

where p_j , ε_j express the momentum and kinetic energy of particle species j ($j = 1, 2, 3$ and 4 refer to B_1, B_2, e

and $\bar{\nu}_e$), respectively. f_j is the Fermi-Dirac distribution functions of baryons and electrons,

$$f_B = \frac{1}{\exp((E_B - \mu_B)/T) + 1}, \quad (19)$$

$$f_e = \frac{1}{\exp((\varepsilon_3 - \mu_e)/T) + 1}.$$

The delta functions $\delta(E_1 - E_2 - \varepsilon_3 - \varepsilon_4)$ and $\delta(\mathbf{p}_1 - \mathbf{p}_2 - \mathbf{p}_3 - \mathbf{p}_4)$ describe the energy and momentum conservation. $E_{1,2} = \varepsilon_{1,2} + U_{1,2}$ is the energy of baryons. $U_{1,2}$ is the potential energy of baryons, which can be obtained in Section A and has the following form

$$U_B = g_{\omega B}\omega_0 + g_{\rho B}I_{3B}\rho_0 + g_{\phi B}\phi_0. \quad (20)$$

Namely,

$$\begin{aligned} U_n - U_p &= -g_{\rho N}\rho_0, \\ U_{\Sigma^-} - U_{\Sigma^0} &= -g_{\rho\Sigma}\rho_0, \\ U_{\Xi^-} - U_{\Xi^0} &= -g_{\rho\Xi}\rho_0. \end{aligned} \quad (21)$$

$|M_{fi}|^2$ is the squared matrix element of the baryon direct Urca processes summed over spins of initial and final particles

$$\begin{aligned} |M_{fi}|^2 &= 32G_F^2 C^2 [(g_1^2 - f_1^2)M_1^* M_2^* (P_4 P_3) + (g_1 - f_1)^2 (P_4 P_2)(P_3 P_1) \\ &\quad + (g_1 + f_1)^2 (P_4 P_1)(P_3 P_2)], \end{aligned} \quad (22)$$

where $P_j = (\varepsilon_j, \mathbf{p}_j)$. $G_F = 1.436 \times 10^{-49}$ erg cm³ is the weak-coupling constant. f_1, g_1 and C are the vector, axial-vector constant and Cabibbo angle which are given in Table III.

The relativistic expression of the energy loss Q per unit volume and time in NS matter is expressed as [46, 47]

$$\begin{aligned} Q &= \frac{457\pi}{10080} G_F^2 C^2 T^6 \Theta (p_{F3} + p_{F2} - p_{F1}) \\ &\quad \times \{f_1 g_1 ((\varepsilon_{F1} + \varepsilon_{F2}) p_{F3}^2 - (\varepsilon_{F1} - \varepsilon_{F2})(p_{F1}^2 - p_{F2}^2)) \\ &\quad + 2g_1^2 \mu_e m_1^* m_2^* + (f_1^2 + g_1^2)(\mu_e (2\varepsilon_{F1}\varepsilon_{F2} - m_1^* m_2^*)) \\ &\quad + \varepsilon_{F1} p_3^2 - \frac{1}{2}(p_{F1}^2 - p_{F2}^2 + p_{F3}^2)(\varepsilon_{F1} + \varepsilon_{F2})\}, \end{aligned} \quad (23)$$

In this expression, p_{F1}, p_{F2} and p_{F3} are the Fermi momenta of baryons and leptons. ε_{F1} and ε_{F2} are the kinetic energy of baryon at the Fermi surface. $\Theta = 1$ if the Fermi momenta p_{F1}, p_{F2}, p_{F3} satisfy the triangle condition and $\Theta = 0$ otherwise. The situation of muons is similar to that of electrons.

The cooling equation based on the approximation of isothermal interior is,

$$C_v \frac{dT}{dt} = -(L_\nu + L_r). \quad (24)$$

Here L_ν and L_r are the total neutrino and photon luminosities, respectively. C_v is the total thermal capacity of NS matter. They are

$$\begin{aligned} L_\nu &= \int Q_0 e^{2\Phi} dV, L_r = 4\pi R^2 \sigma (10T)^{\frac{8}{3}} e^{2\Phi_s}, \\ C_{v0} &= \int (C_e + C_\mu + \sum_B C_{B0}) dV, \end{aligned} \quad (25)$$

where σ is the Stefan-Boltzmann constant, $e^\Phi = \sqrt{1 - 2m/r}$ is the gravitational redshift. e^{Φ_s} is the value of e^Φ at the stellar surface ($r=R$). The semiempirical expression $T_s = (10T)^{2/3}$ expresses the relation between interior temperature T and surface temperature T_s .

C. SF of protons

The key quantity in determining the onset of 1S_0 proton SF is the gap function $\Delta(p)$,

$$\Delta(p) = -\frac{1}{4\pi^2} \int p'^2 dp' \frac{V(p, p') \Delta(p')}{\sqrt{\varepsilon^2(p') + \Delta^2(p')}}, \quad (26)$$

where $\varepsilon(p) = E(p) - E(p_{Fp})$. $E(p)$ is the single-particle energy of protons with momentum p

$$E(p) = \sqrt{p^2 + m_p^{*2}} + g_{\omega p}\omega + g_{\phi p}\phi + g_{\rho p}I_{3p}\rho. \quad (27)$$

$V(p, p')$ is the pp potential matrix element. In this work, we use the Reid soft core(RSC) potential for the pp potential[48–51], as an example to demonstrate the influence of hyperons on the 1S_0 proton pairing energy gaps. The critical temperature T_{cp} of 1S_0 proton SF is given by the pairing gap $\Delta(k)$ at zero temperature approximation,

$$T_{cp} \doteq 0.57\Delta(k). \quad (28)$$

As a result, the neutrino emissivity and thermal capacity can be written as

$$Q = Q_0 R_B, \quad C_B = C_{B0} R_{C_{B0}}. \quad (29)$$

Here R_B and $R_{C_{B0}}$ are the SF reduction factors of the neutrino emissivity and thermal capacity, respectively. For the 1S_0 proton SF, the reduction factors R_p and $R_{C_{p0}}$ are

$$R_p = \frac{0.0163 \exp(\frac{-1.764T_{cp}}{T})}{(\frac{T}{T_{cp}})^{5.5}}, R_{C_{p0}} = \frac{3.149 \exp(\frac{-1.764T_{cp}}{T})}{(\frac{T}{T_{cp}})^{2.5}}. \quad (30)$$

According to the discussion of the RMF approach above, we can obtain the EOS, mass-radius relations and neutrino emissivities of the reactions A, B, C as well as Fermi momentum and single particle energy of protons, then the pairing gap and critical temperature of 1S_0 proton SF and speed of the NS cooling can be obtained.

III. RESULTS AND DISCUSSION

In this section, we give three cases in Eq.(1) for RMF theory: (i) the non-strange σ, ω, ρ mesons are included in SU(6) spin-flavor symmetry; (ii) the σ, ω, ρ mesons including strange mesons σ^* and ϕ are considered in SU(6) spin-flavor symmetry; (iii) $\sigma, \omega, \rho, \sigma^*$ and ϕ mesons are

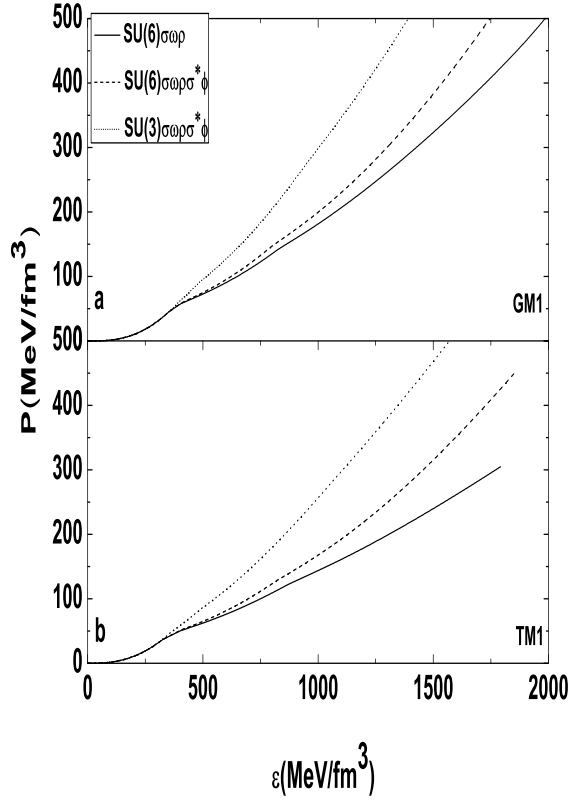


FIG. 1. EOSs including hyperons in NS matter.

taken into account in SU(3) flavor symmetry. We mainly study the effects of the degrees of freedom of hyperons and reactions B, C on the EOS, neutrino emissivity, neutrino luminosity, energy gap of 1S_0 proton SF and NS cooling. Then we compare our results with PSR J1614-2230 and J0348+0432, whose measured masses are used as reference values.

Fig. 1 shows the EOSs in three cases. Fig. 2 shows the mass-radius relations of NSs by solving the TOV equation. The softest and hardest EOSs are obtained by cases (i) and (iii), respectively. Though the coupling $g_{\omega N}$ for case (iii) is smaller than the corresponding value for case (i) as shown in Table 1, the total repulsive force is attributed not only to ω meson but also to ϕ meson. As seen in Fig. 1 and 2, though we consider the contribution of the strange mesons σ^* and ϕ on the EOS in case (ii), the coupling $g_{\phi N}=0$. It means that ϕ meson only couples to hyperons and makes the EOS be not enough stiff. So the hardest EOS is obtained only through the ϕ meson in case (iii). From case (i) to (iii), the maximum mass of NS (the corresponding center density) sequentially increases from $1.820 (0.771)$, $1.863 (0.817)$ to $2.141M_{\odot} (0.871)$ for the GM1 model, $1.686 (0.673)$, $1.729 (0.754)$ to $2.038M_{\odot} (0.848)$ for the TM1 model, respectively (Fig.

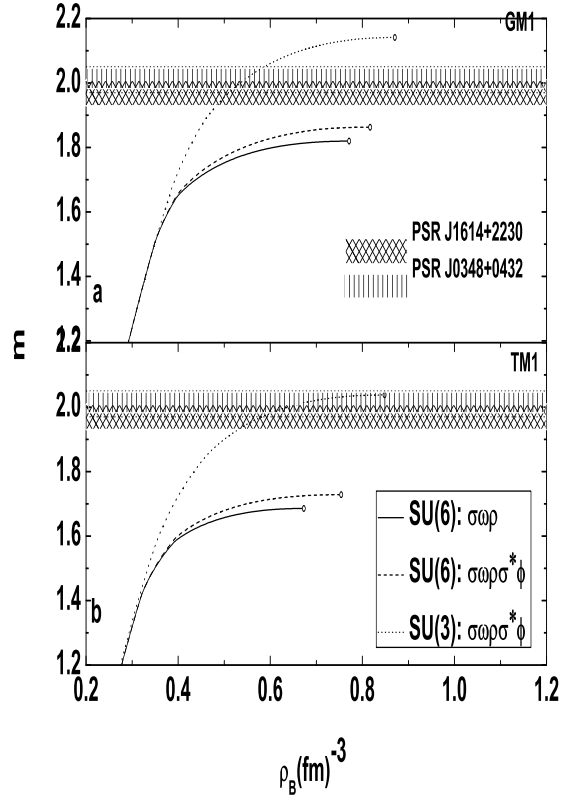


FIG. 2. Mass-radius relations including hyperons.

2). Namely, the EOS in SU(3) flavor symmetry could be consistent with the observed values of PSR J1614-2230 and J0348+0432 when hyperons appear in NS core. Fig. 3 depicts the neutrino emissivities of the reactions A, B, C in $nphe\mu$ matter for the three cases. In order to make the effects of hyperons and reactions B, C on A more intuitive, Fig. 4 depicts the total neutrino emissivity of the reactions A, B, C in $npe\mu$ and $nphe\mu$ matter for case (iii). As can be seen from Figs. 3 and 4, the neutrino emissivity of the reaction A has a tendency to decrease with increasing of the baryon density ρ_B due to the presence of hyperons in NS matter decreases the nucleon and lepton fractions according to the requirement of the charge neutrality and β equilibrium conditions (Eqs.(12) and (13)). Also, the neutrino emissivities of the reactions B and C are obviously less than that of A, it is due to that they have smaller matrix elements in Eq.(22). The strongest neutrino emissivity of the reaction A or B is in case (iii), while the weakest one is observed in case (i). For the reaction C, the neutrino emissivity in case (iii) is less than the corresponding values in cases (i) and (ii) firstly and then increases slowly, equals or exceeds the values in cases (i) and (ii). While the reactions D-F would never happen within stable NSs, because their threshold densi-

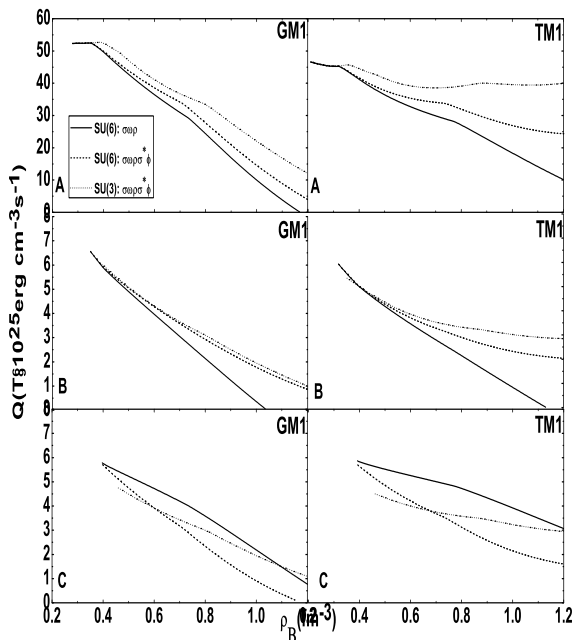


FIG. 3. Neutrino emissivities of the reactions A, B and C as a function of the baryon density ρ_B in $npe\mu$ matter.

ties are larger than the center densities of maximum mass NSs. As shown in Figs. 2 and 3, the mass ranges of the reactions B and C in case (iii) are $1.671 - 2.141M_\odot$ and $1.888 - 2.141M_\odot$ for the GM1 model, $1.579 - 2.038M_\odot$ and $1.849 - 2.038M_\odot$ for TM1 model, respectively.

Next we mainly discuss the effects of the degrees of freedom of hyperons and reactions B, C on the total neutrino emissivity, neutrino luminosity, energy gap of 1S_0 proton SF and NS cooling in case (iii). Fig. 5 gives the radial distributions of the total neutrino emissivities of the reactions A, B, C for the GM1 model with 1.98, 2.00, 2.10, 2.12 M_\odot stars in case (iii). The radial distributions of the total neutrino emissivity for the same mass stars in $npe\mu$ and $nphe\mu$ matter are almost unchanged when r is relatively large (Part I). However, the reactions B and C happen in succession as the radius decreases (Part II and III), leading to the radial distributions of the total neutrino emissivities in $nphe\mu$ matter are significantly larger than the values in $npe\mu$ matter. While the radius regions of the increasing total neutrino emissivities shrink continually with the increasing NS mass. The situation of the TM1 model is like the above in GM1 model. Fig. 6 shows the total neutrino luminosity as a

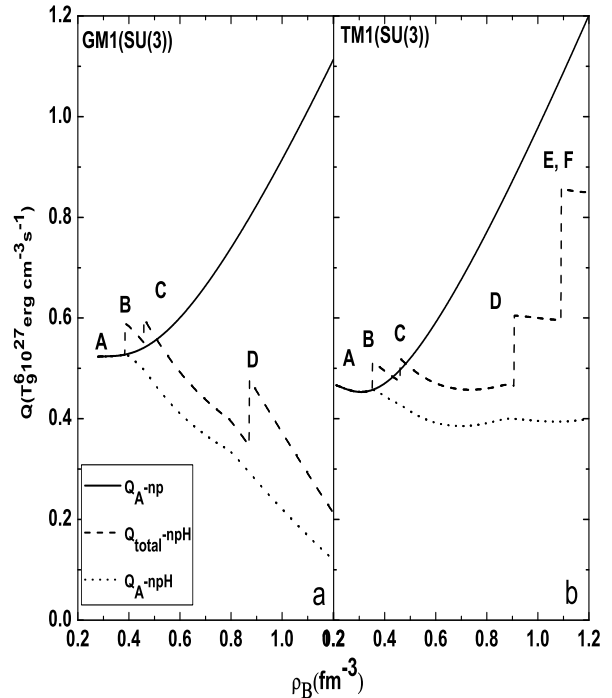


FIG. 4. Total neutrino emissivities of the reactions A-F as a function of the baryon density ρ_B . The solid line is the neutrino emissivity of the reaction A in $npe\mu$ matter. The dashed line is the total neutrino emissivity of the reactions A-F in $nphe\mu$ matter. The dotted line is the neutrino emissivity of the reaction A in $nphe\mu$ matter.

function of NS mass m in case(iii). As seen from Fig. 6, whether hyperons are included or not, the neutrino luminosity increases firstly and then decreases with the increasing of the baryon density ρ_B . Once the mass of NS reaches a value, one luminosity corresponds to two different NSs. And the total neutrino luminosities of reactions A, B, C within the mass range $1.603 - 2.067M_\odot$ and $1.515 - 1.840M_\odot$ will be larger than the values in $npe\mu$ matter for the GM1 and TM1 models, respectively. Fig.7 shows the 1S_0 proton SF critical temperatures as a function of the baryon density ρ_B for case(iii) in $npe\mu$ matter (solid lines) and $nphe\mu$ matter (dashed lines), respectively. One can find that whether or not the NS core appears hyperons, the 1S_0 proton SF critical temperature first increases, reaches a peak and then decreases to zero as the baryon density ρ_B increases. While when the NS core appears hyperons, the 1S_0 proton SF critical temperatures are first below and then above the corresponding values in $npe\mu$ matter within the density ranges of $\rho_B = 0.0 - 0.454 \text{ fm}^{-3}$ ($\rho_B = 0.0 - 0.418 \text{ fm}^{-3}$ for the TM1 model) and $\rho_B \geq 0.454 \text{ fm}^{-3}$ ($\rho_B \geq 0.418 \text{ fm}^{-3}$ for the TM1 model) for the GM1 model, respectively. It is because the total contribution of the Fermi momentum

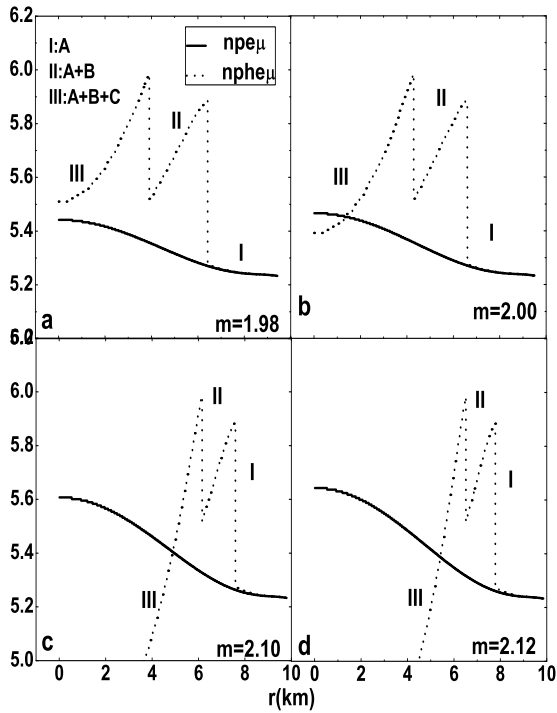


FIG. 5. Radial distributions of the total neutrino emissivities with different mass NSs in $npe\mu$ matter (solid lines) and $nphe\mu$ matter (dotted lines) in the GM1 model

and single-particle energy of protons (see Eqs.(11) and (27)) results in T_{CP} change. Besides, the density range of the 1S_0 proton SF is widened due to the inclusion of hyperons. The range of 1S_0 proton SF can achieve coverage or partial coverage in the cores of NSs, which is highly relevant to the reactions A, B. That is, the presence of hyperons affects not only the reaction A and 1S_0 proton SF critical temperature, but also the NS cooling. In Figs. 8 and 9, the cooling curves of NSs are calculated through solving the cooling Eq.(24) by assuming isothermal NS cores for case(iii). Observational data of 8 isolated NSs whose effective surface temperatures have been measured or constrained are listed as compared with the theoretical cooling curves [52–61]. As you can see from Figs. 8 and 9, the cooling curves of moderate mass NSs can explain the observational data, while the cooling curves for massive NSs due to the low surface temperature are difficult to explain the existing observational data. And the cooling curves decrease smoothly with the increasing NS mass, meaning that the cooling of massive NSs undergoes faster neutrino cooling whether the reactions B and C appear in NSs. In addition, the same mass stars with

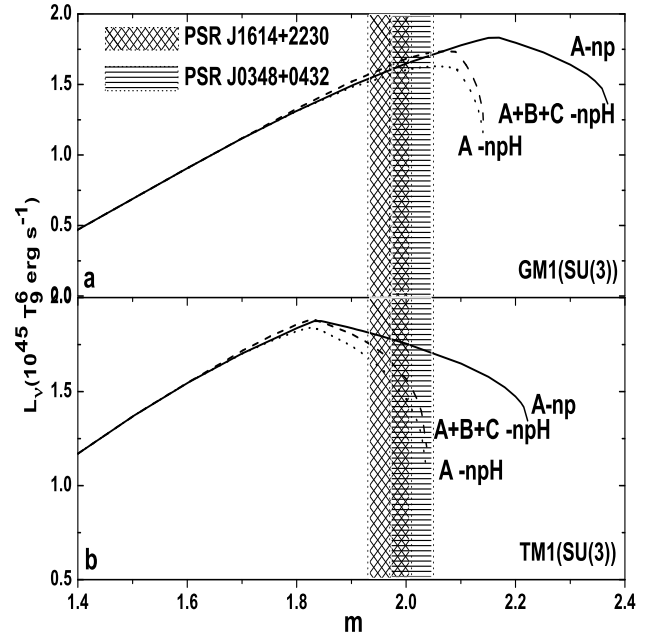


FIG. 6. Total neutrino luminosity of the reactions A, B, C as a function of the NS mass m . The solid line is the neutrino luminosity of the reaction A in $npe\mu$ matter. The dashed line is the total neutrino luminosity of the reactions A, B, C in $nphe\mu$ matter. The dotted line is the neutrino luminosity of the reaction A in $npe\mu$ matter.

the reactions B, C (dashed lines) are colder than that in $npe\mu$ matter (solid lines). Taking case (iii) in GM1 model as an example, we can see that the neutrino luminosity of 1.70, 1.95, 2.03 M_\odot NSs in $nphe\mu$ matter are greater than the corresponding values in $npe\mu$ matter which is because the three NSs within the mass range 1.671 – 2.067 M_\odot , see Fig. 6 for details. While the 1S_0 proton SF critical temperatures T_{CP} of 1.70, 1.95, 2.03 M_\odot in $nphe\mu$ matter is lower than the value in $npe\mu$ matter (see Figs. 2 and 7 for details), in the case we studied here. As a result, the reactions A, B are suppressed in advance in $nphe\mu$ matter. However, the reaction C is not affected by the 1S_0 proton SF. Therefore, although the neutrino emissivities of the reactions A and B are suppressed with the presence of the 1S_0 proton SF, the total contribution of reactions A, B, C can still speed up a massive NS cooling. For the TM1 model, the situation is similar to the described in GM1 model. The cooling curves presented here are estimates in order to make the effects of the 1S_0 proton SF on the reactions A and B be more clearly, in particular, the effects of NS crust and hyperons SF are not considered.

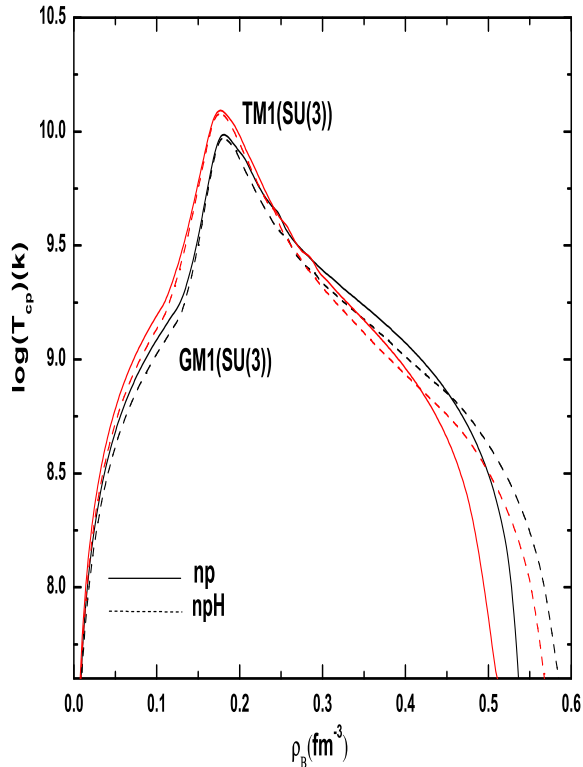


FIG. 7. The critical temperature T_{cp} of the 1S_0 proton SF as a function of the NS mass m in $npe\mu$ matter (solid lines) and $nphe\mu$ matter (dashed lines)

IV. CONCLUSION

We have studied the effects of the degrees of freedom of hyperons and reactions B, C on the reaction A in NS matter using the two popular RMF parameter sets, GM1 and TM1, respectively. Firstly, we used the SU(3) flavor symmetry to obtain the relatively stiff EOS for supporting the observed massive PSR J1614-2230 and J0348+0432. Secondly, the total neutrino luminosity of the reactions A, B, C are calculated in $npe\mu$ and $nphe\mu$ matter, respectively. We found that the presence of the reactions B and C caused of the total neutrino luminosity higher than the corresponding values in $npe\mu$ matter within the mass range $1.603 - 2.067M_\odot$ for the GM1 model and $1.515 - 1.840M_\odot$ for the TM1 model. Finally, our main

purpose is to test the effects of the 1S_0 proton SF on the reactions A, B by comparing cooling curves with observed data. We will analyze the effects of other baryon SF on the corresponding baryon direct Urca processes in future work. Our results showed that the cooling rate of the same mass of two NSs with the reactions B and C are obviously faster than that without the reactions B and

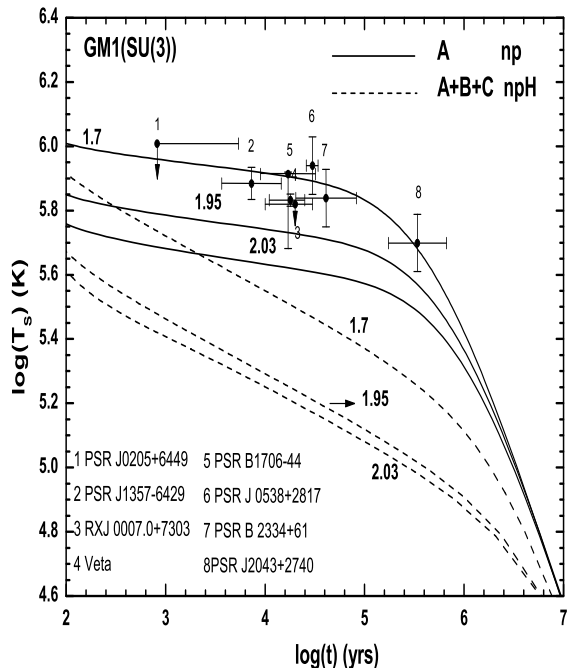


FIG. 8. Observational data (error bars) on surface temperatures of 8 NSs as compared with theoretical cooling curves obtained by the GM1 model for proton SF from Fig.7. The solid lines correspond to $npe\mu$ matter, the dashed lines correspond to $nphe\mu$ matter with masses (from top to bottom) $1.5, 1.7, 1.95$ and $2.03M_\odot$, respectively.

C. These features maybe can help to prove the presence of hyperons in massive NSs cores.

ACKNOWLEDGMENTS

This work is funded by the National Natural Science Foundation of China (Grant Nos. 11447165, 11373047, U14311121, 11265009) and Youth Innovation Promotion Association, CAS (Grant Nos. 2016056).

[1] D. G. Yakovlev, C. J. Pethick, *Ann. Rev. Astron. Astrophys.* **42**, 169(2004).
 [2] D. G. Yakovlev et al., *AIP Conf. Series* **983**, 379(2008).

[3] C. R. Ji, D. P. Min, *Phys. Rev. D* **57**, 5963(1998).
 [4] D. G. Yakovlev, K. P. Levenfish, Y. A. Shibano, *Phys. Uspek* **42**, 737(1999).

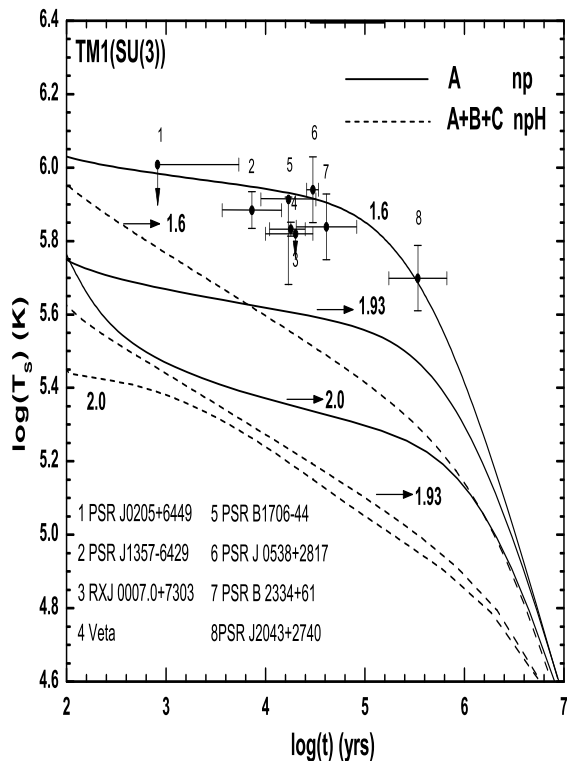


FIG. 9. Observational data(error bars) on surface temperatures of 8 NSs as compared with theoretical cooling curves obtained by the TM1 model for proton SF from Fig.7. The solid lines correspond to $np\mu$ matter, the dashed lines correspond to $nphe\mu$ matter with masses(from top to bottom) 1.4, 1.6, 1.93 and $2.0M_{\odot}$, respectively.

- [5] E. G. Zhao, F. Wang, Chin. Sci. Bull **56**, 3797(2011).
 [6] Z. F. Gao et al. Ap & SS **334**, 281(2011).
 [7] H. Sotani, T. Maruyama, T. Tatsumi, Nucl. Phys. A **906**, 37(2013).
 [8] C. Schaab, S. Balberg, J. Schaffner-Bielich, Astrophys. J **504**, L99(1998).
 [9] Y. N. Wang, H. Shen, Phys. Rev. C **81**, 025801(2010).
 [10] Y. Xu et al., Research in Astron. Astrophys **15**, 725(2015).
 [11] S. Tsuruta, Phd. Thesis, Columbia University(1964).
 [12] E. Flowers, M. Ruderman, P. Sutherland, Astrophys. J **205**, 541(1976).
 [13] O. V. Maxwell, Astrophys. J **231**, 201(1979).
 [14] E. H. Gudmundsson, C. J. Pethick, R. I. Epstein, Astrophys. J **272**, 286(1983).
 [15] D. Page, J. H. Applegate, Astrophys. J **394**, 17(1992).
 [16] A. D. Kaminker, P. Haensel, D. G. Yakovlev, Astron. Astrophys **373**, L17(2001).
 [17] D. G. Yakovlev et al., Nucl. Phys. A **752**, 90(2005).
 [18] C. Kouvaris, Phys. Rev. D **77**, 023006(2008).
 [19] D. Blaschke, H. Grigorian, D. N. Voskresensky, F. Weber, Phys. Rev. C **85**, 022802 (2012).
 [20] M. V. Beznogov, D. G. Yakovlev, Mon. Not. R. Astron. Soc **447**, 1598(2015).
 [21] J. M. Lattimer, C. J. Pethick, M. Prakash, P. Haensel, Phys. Rev. Lett **66**, 2701(1991).
 [22] M. Prakash et al., Astrophys. J **390**, 77(1992).
 [23] P. Haensel, O. Y. Gnedin, Astron. Astrophys **290**, 458(1994).
 [24] K. P. Levenfish, D. G. Yakovlev, Astron. Lett **20**, 43(1994).
 [25] M. E. Gusakov, Astron. Astrophys **389**, 702(2002).
 [26] Y. Xu et al., Chin. Phys. Lett **28**, 079701(2011).
 [27] Y. Xu et al., Commun. Theor. Phys **56**, 521(2011).
 [28] Y. Xu et al., Chin. Sci. Bull **59**, 273(2014).
 [29] J. Boguta, A. R. Bodmer, Nucl. Phys. A **292**, 413(1977).
 [30] J. Boguta, Phys. Lett. B **106**, 250(1981).
 [31] J. Boguta, H. Stocker, Phys. Lett. B **120**, 289(1983).
 [32] W. Pannert, P. Ring, J. Boguta, Phys. Rev. L **59**, 2420(1987).
 [33] J. Schaffner, I. N. Mishustin, Phys. Rev. C **53**, 1416(1996).
 [34] F. Yang, H. Shen, Phys. Rev. C **77**, 025801(2008).
 [35] Y. Xu et al., Chin. Phys. Lett **30**, 129501(2013).
 [36] P. B. Demorest et al., Nature **467**, 1081(2010).
 [37] J. Antoniadis et al., Science **340**, 448 (2013).
 [38] S. Weissenborn, D. Chatterjee, J. Schaffner-Bielich, Phys. Rev. C **85**, 065802(2012).
 [39] T. Miyatsu, M. K. Cheoun, K. Saito, Phys. Rev. C **88**, 015802(2013).
 [40] S. Weissenborn, D. Chatterjee, J. Schaffner-Bielich, Nucl. Phys. A **914**, 421(2013).
 [41] L. L. Lopes, D. P. Menezes, Phys. Rev. C **89**, 025805(2014).
 [42] T. Takatsuka, R. Tamagaki, Nucl. Phys. A **738**, 387(2004).
 [43] Y. Xu, et al., Chin. Phys. Lett **29**, 059701(2012).
 [44] J. R. Oppenheimer, G. M. Volkoff, Phys. Rev **55**, 3741939.
 [45] R. C. Tolman, Phys. Rev **55**, 364(1939).
 [46] L. B. Leinson, A. Pérez, Phys. Lett. B **518**, 15(2001).
 [47] Leinson, L. B., Nucl. Phys. A **707**, 543(2002).
 [48] D. W. L. Sprung, P. K. Banerjee, Nucl. Phys. A **168**, 273(1971).
 [49] L. Amundsen, E. Østgaard, Nucl. Phys. A **437**, 487 (1985).
 [50] S. Nishizaki, T. Takatsuka, N. Yahagi, J. Hiura, Prog. Theor. Phys **86**, 853(1991).
 [51] J. Wambach, T. L. Ainsworth, D. Pines, Nucl. Phys. A **555**, 128(1993).
 [52] P. Slane et al., Astrophys. J **616**, 403(2004).
 [53] V. E. Zavlin, astro-ph/0702426(2007).
 [54] V. E. Zavlin, Astrophys. J **665**, L143(2007).
 [55] J. P. Halpern et al., Astrophys. J **612**, 398(2004).
 [56] G. G. Pavlov et al., Astrophys. J **552**, 129(2001).
 [57] K. E. McGowan et al., Astrophys. J **600**, 343(2004).
 [58] V. E. Zavlin, G. G. Pavlov, Mem. Soc. Astron. Ital **75**, 458(2004).
 [59] A. Possenti, S. Mereghetti, M. Colpi, Astron. Astrophys **313**, 565(1996).
 [60] O. Y. Kargaltsev et al., Astrophys. J **625**, 307(2005).
 [61] W. C. G. Ho et al., Astrophys. J **375**, 821(2007).